Title

Combined CDK4/6 and Pan-mTOR Inhibition Is Synergistic Against Intrahepatic Cholangiocarcinoma

Journal

Clinical Cancer Research, 25(1)

ISSN

1078-0432

Authors

Song, Xinhua
Liu, Xianqiong
Wang, Haichuan
et al.

Publication Date

2019

DOI

10.1158/1078-0432.ccr-18-0284

Peer reviewed

HHS Public Access

Author manuscript

Clin Cancer Res. Author manuscript; available in PMC 2020 January 01.

Published in final edited form as:

Clin Cancer Res. 2019 January 01; 25(1): 403–413. doi:10.1158/1078-0432.CCR-18-0284.

Combined CDK4/6 and pan-mTOR inhibition is synergistic against intrahepatic cholangiocarcinoma

Xinhua Song[1,2], **Xianqiong Liu**[2,3], **Haichuan Wang**[2,4], **Jingxiao Wang**[2,5], **Yu Qiao**[2,6], **Antonio Cigliano**[7], **Kirsten Utpatel**[8], **Silvia Ribback**[7], **Maria G. Pilo**[7], **Marina Serra**[7], **John D. Gordan**[9], **Li Che**[2], **Shanshan Zhang**[2], **Antonio Cossu**[10], **Alberto Porcu**[11], **Rosa M. Pascale**[11], **Frank Dombrowski**[7], **Hongbo Hu**[1], **Diego F. Calvisi**[7], **Matthias Evert**[8], and **Xin Chen**[2]

[1]Beijing Advanced Innovation Center for Food Nutrition and Human Health, College of Food Science and Nutritional Engineering, China Agricultural University, Beijing, China

[2]Department of Bioengineering and Therapeutic Sciences and Liver Center, University of California, San Francisco, CA, USA

[3]School of Pharmacy, Hubei University of Chinese Medicine Wuhan, Hubei, China

[4]Department of Liver Surgery, Liver Transplantation Division, West China Hospital, Sichuan University, Chengdu, China

[5]Beijing University of Chinese Medicine, Beijing, China

[6]Department of Oncology, Beijing Hospital, Beijing, China

[7]Institute of Pathology, University of Greifswald, Greifswald, Germany

[8]Institute of Pathology, University of Regensburg, Regensburg, Germany

[9]Department of Medicine, University of California, San Francisco, CA, USA

[10]Unit of Pathology, Azienda Ospedaliero Universitaria Sassari, Sassari, Italy

[11]Department of Clinical and Experimental Medicine, University of Sassari, Sassari, Italy

Abstract

Purpose: Intrahepatic cholangiocarcinoma (ICC) is an aggressive cancer type, lacking effective therapies and associated with a dismal prognosis. Palbociclib is a selective CDK4/6 inhibitor, which has been shown to suppress cell proliferation in many experimental cancer models. Recently, we demonstrated that pan-mTOR inhibitors, such as MLN0128, effectively induce apoptosis, while having limited efficacy in restraining proliferation of ICC cells. Here, we tested the hypothesis that Palbociclib, due to its ant-proliferative properties in many cancer types, might synergize with MLN0128 to impair ICC growth.

Corresponding authors: Hongbo Hu, Beijing Advanced Innovation Center for Food Nutrition and Human Health, College of Food Science and Nutritional Engineering, China Agricultural University, No. 17 Qinghua East Road, Haidian District, Beijing 100083, China; phone: +86 (10) 62378653; hongbo@cau.edu.cn; Matthias Evert, Institut für Pathologie, Universitätsklinikum Regensburg, Franz-Josef-Strauß-Allee 11, 93053 Regensburg, Germany; phone: +49 0941 944-6600; fax: +49 0941 944-6602; Matthias.Evert@ukr.de; Xin Chen, UCSF, 513 Parnassus Avenue, San Francisco, CA 94143, U.S.A. Phone: +1 415 502-6526; xin.chen@ucsf.edu.

Competing interests: The authors have no conflict of interest.

Experimental Design: Human ICC cell lines and the AKT/YapS127A ICC mouse model were used to test the therapeutic efficacy of Palbociclib and MLN0128, either alone or in combination.

Results: Administration of Palbociclib suppressed *in vitro* ICC cell growth by inhibiting cell cycle progression. Concomitant administration of Palbociclib and MLN0128 led to a pronounced, synergistic growth constraint of ICC cell lines. Furthermore, while treatment with Palbociclib or MLN0128 alone resulted in tumor growth reduction in AKT/YapS127A mice, a remarkable tumor regression was achieved when the two drugs were administered simultaneously. Mechanistically, Palbociclib was found to potentiate MLN0128 mTOR inhibition activity, whereas MLN0128 prevented the upregulation of cyclin D1 induced by Pa1bociclib treatment.

Conclusions: Our study indicates the synergistic activity of Palbociclib and MLN0128 in inhibiting ICC cell proliferation. Thus, combination of CDK4/6 and mTOR inhibitors might represent a novel, promising, and effective therapeutic approach against human ICC.

Keywords

Targeted therapies; Precision medicine; Intrahepatic cholangiocarcinoma; Palbociclib; MLN0128

Introduction

Intrahepatic cholangiocarcinoma (ICC) is the second most frequent form of primary liver cancer after hepatocellular carcinoma (HCC) (1–3). Epidemiologic data indicate a steady increase of ICC incidence over the past decades worldwide (1). Most ICC patients do not show early symptoms and are often diagnosed at advanced stages, thus precluding potentially effective therapies such as surgical resection or liver transplantation (4). The median survival time of patients with unresectable ICC without treatment is shorter than 5 months, and it can be expanded up to ~ 1 year by systemic chemotherapy (5). The combination of gemcitabine and platin-based drugs is the standard first line treatment for patients with advanced or metastatic ICC (2). However, this regimen has very limited therapeutic value, with drug-resistance rapidly developing (2). Thus, new and effective therapeutic strategies are urgently needed for this lethal malignancy.

Deregulation of cell cycle induces unconstrained cell division, which leads to continuous proliferation and represents a crucial driver of carcinogenesis (6–8). The cyclin/cyclin-dependent kinase (CDK)/retinoblastoma (Rb) axis is an important regulator of the cell cycle (9). In physiological conditions, unphosphorylated (active) Rb protein (encoded by the *Rb1* gene) blocks cell cycle progression by sequestrating the E2F1 transcription factor through physical interaction (10). In cancer cells, mitogens and cytokines trigger the upregulation of the Cyclin D1 (CCND1) protein. Subsequently, CCND1, in complex with CDK4/6, inactivates the Rb protein via phosphorylation at multiple serine residues (10,11). Consequently, the ability of Rb to repress E2F1 is impaired, resulting in the induction of E2F target genes, which are responsible for G1-S transition and, thus, unconstrained cell proliferation (10). In light of this body of evidence, it is not surprising that cell cycle inhibitors have been developed and shown to be effective against various cancer types (12). Among these inhibitors, Palbociclib is a highly selective and orally-active CDK4/6 suppressor able to induce cell cycle arrest *in vitro* and *in vivo* (6,13). To date, Palbociclib has

demonstrated significant antineoplastic activity on multiple tumor entities, including human breast, colon, lung, and bladder cancers, as well as hepatocellular carcinoma and leukemia, which are all characterized by an intact *Rb1* gene (14–16). The importance of Palbociclib as a clinically relevant anti-tumor drug is underscored by its approval from the US Food and Drug Administration (FDA) for the treatment of hormone receptor-positive/HER2-negative advanced breast cancer (17). Although ICC is rarely affected by genetic alterations at the *Rb1* gene and its locus (18), the therapeutic significance of Palbociclib or other CDK4/6 inhibitors for ICC treatment has not been determined so far.

Phosphoinositide-3-kinase (PI3K)/v-AKT murine thymoma viral oncogene homolog (AKT)/mammalian target of rapamycin (mTOR) cascade is a critical pathway regulating various cellular processes including cell proliferation, survival, and metabolism, and is implicated in cancer development and/or progression (19). Aberrant activation of the PI3K/AKT/mTOR cascade has been detected in most human ICCs (20,21). MLN0128 is a second-generation pan-mTOR inhibitor, possessing significant anti-cancer growth activity on multiple tumor types (22). MLN0128 is currently under evaluation in several Phase I and II clinical trials as a single agent or in combination therapy (https://clinicaltrials.gov/). In a recent study, using a murine ICC model induced by activated/oncogenic forms AKT and Yap (AKT/YapS127A), we found that MLN0128 treatment results in a stable disease (21). Mechanistically, MLN0128 induced elevated cell apoptosis in AKT/YapS127A cholangiocellular lesions, while only marginally affecting their proliferation properties (21).

Here, we determined whether Palbociclib administration possesses anti-proliferative proliferative activity towards ICC cells *in vitro* and *in vivo*. In addition, we evaluated whether Palbociclib synergizes with the mTOR inhibitor MLN0128 to induce ICC regression. For this purpose, Palbociclib and MLN0128, either alone or in combination, were administered to ICC cell lines and AKT/YapS127A mice. Noticeably, while treatment with Palbociclib alone slowed ICC proliferation, the combination therapy had a striking effect in inhibiting tumor growth. At the cellular level, the enhanced growth constraint achieved by Palbociclib/MLN0128 combination was mainly due to strong inhibition of tumor cell proliferation. To our knowledge, this is the first body of evidence demonstrating the important therapeutic effect of Palbociclib and, particularly, Palbociclib/MLN0128 combination, on ICC growth *in vitro* and *in vivo*. Thus, the present study underlines the anti-neoplastic efficay of Palbociclib/MLN0128 treatment in experimental models of ICC, envisaging its usefulness as a new therapeutic option for the human disease.

Materials and Methods

In vitro studies.

The human KKU-M213, huCC-T1, SNU1196, and MzChA-1 ICC cell lines, after validation (Genetica DNA Laboratories, Burlington, NC), were used in the study. Cells were grown in a 5% CO_2 atmosphere, at 37˚C, in RPMI Medium supplemented with 10% fetal bovine serum (FBS; Gibco, Grand Island, NY) and penicillin/streptomycin (Gibco). All experiments were repeated at least three times.

Constructs and Reagents.

The constructs used for mouse injection, including pT3-EF1α, pT3-EF1α-HA-myr-AKT (mouse), pT3-EF1α-YapS127A (human), and pCMV/sleeping beauty transposase (SB) have been described previously (23–25). Plasmids were purified using the Endotoxin free Maxi Prep Kit (Sigma-Aldrich, St. Louis, MO) before injection. Palbociclib (LC Laboratories, Woburn, MA) was formulated in 0.5% Tween 80 and 0.5% carboxymethylcellulose (CMC) in purified water to a concentration of 20 mg/ml and stored at −20▒. MLN0128 (LC Laboratories) was dissolved in NMP (1-methyl-2-pyrrolidinone; Sigma-Aldrich) to generate a stock solution of 20 mg/ml. It was diluted 1:200 into 15% PVP/H_2O (PVP: polyvinylpyrrolidone K 30, Sigma-Aldrich; diluted in H_2O at a 15.8:84.2 w/v ratio) before administration to the mice. Palbociclib and MLN0128 were dissolved in DMSO for *in vitro* experiments.

In vitro cell culture, colony formation assay, and IC_{50} determination.

Eight human ICC cell lines (KKU-M213, huCC-T1, SNU1196, MzChA-1, RBE, TGBC, OCUG-1 and KMCH) were used for *in vitro* studies. Cell lines were maintained as monolayer cultures in Dulbecco's modified Eagle medium supplemented with 10% fetal bovine serum (FBS, Gibco, Grand Island, NY, USA), 100 U/ml penicillin, and 100 g/ml streptomycin (Gibco). For colony formation assay, cells were plated in 6-well culture plates at a density of 0.5–1 × 10^3 cells/well when cells reached 70–80% confluency in 60 × 15 mm culture dishes and treated with indicated doses of Palbociclib. Equivalent amounts of DMSO treated cells were used as control. Two-three weeks later, colonies were stained with crystal violet and then counted for quantification and colony formation IC50 determination. For IC_{50} determination in short-term Palbociclib treatment, cells were seeded in 96-well plates and treated with increasing doses of Palbociclib in triplicate for 72 hours. Subsequently, cells were tested by Brdu Cell Proliferation kit (Merk Millipore). OD was measured at 450 nm with the BioTek ELx808 Absorbance Microplate Reader (Thermo Fisher Scientific, Waltham, MA).

BrdU incorporation and flow cytometric analysis.

For the BrdU incorporation assay, control or drug-treated cells were incubated with bromodeoxyuridine (BrdU) for 1 hour and the assay was performed using the FITC BrdU Flow Kit (BD Biosciences, San Jose, CA), following the manufacturer's instructions. Briefly, the cells were fixed after removing the medium with BrdU. Then, DNase was used to expose incorporated BrdU. Next, the anti-BrdU antibody was added and bound to newly synthesized cellular DNA, which is labelled with BrdU. 7-AAD was used for the total DNA staining. Measurement of cell cycle parameters was performed with the Becton Dickinson LSRII Flow Cytometer (BD Biosciences) and data processed using the FlowJo 10 software (FlowJo, LLC, Ashland, OR).

Quantitative reverse transcription real-time polymerase chain reaction (qRT-PCR).

Validated Gene Expression Assays for human *Rb1* (ID # Hs01078066_m1), *CDK4* (ID # Hs00364847_m1), *CDK6* (*ID #* Hs01026371_m1), *E2F1* (ID # Hs00153451_m1), *Cyclin* E/CCNE1 (ID # Hs01026536_m1), and *β*-Actin (ID # 4333762T) genes were purchased from

Applied Biosystems (Foster City, CA). PCR reactions were performed with 100 ng of cDNA of the collected samples or cell lines, using an ABI Prism 7000 Sequence Detection System with TaqMan Universal PCR Master Mix (Applied Biosystems). Cycling conditions were: denaturation at 95°C for 10 min, 40 cycles at 95°C for 15 s, and then extension at 60°C for 1 min. Quantitative values were calculated by using the PE Biosystems Analysis software and expressed as N target (NT). $NT = 2^{-\Delta Ct}$, wherein ΔCt value of each sample was calculated by subtracting the average Ct value of the target gene from the average Ct value of the *β- Actin* gene.

Determination of the Combination Index (CI).

The nature of the combinatory effects of Palbociclib and MLN0128 was quantitatively evaluated by the Chou−Talalay method (26,27). Cells were exposed to various doses of Palbociclib and/or MLN0128. The overall suppressive actions were used to calculate the CI using the following formula: $CI = \frac{CA,\ x}{ICx,\ A} + \frac{CB,\ x}{ICx,\ B}$

where CA, x and CB, x are the doses of each compound alone used in combination to produce x% inhibitory action and ICx, A and ICx and B are the doses for each compound alone to produce the same action. CI < 1 indicates a synergistic effect by the combination, whereas CI = 1 means an additive effect. If CI is greater than 1, it suggests antagonism produced by the combination.

Hydrodynamic Injection, Mouse Treatment, and Histopathological Analysis.

Female wild-type (WT) FVB/N mice were obtained from Charles River Laboratories (Wilmington, MA). Hydrodynamic injection was performed as described previously in detail (28). To generate the ICC model, 20μg pT3-EF1α-HA-myr-AKT and 30μg pT3-EF1α-YapS127A and 2μg pCMV/SB were injected in FVB/N mice. MLN0128 (0.5mg/kg/day), Palbociclib (100mg/kg/day), MLN0128 + Palbociclib or vehicle were orally administered via gavage. For early stage MLN0128 therapy model, therapy began 3.5 weeks post injection for 3 consecutive weeks, and mice were sacrificed 6.5 weeks after hydrodynamic injection. For histopathological analysis, liver specimens were fixed in 4% paraformaldehyde and embedded in paraffin. Sections were done at 5 μm in thickness. Preneoplastic and neoplastic liver lesions were assessed by two board-certified pathologists and liver experts (M.E. and K.U.). Mice were housed, fed, and monitored in accordance with protocols approved by the Committee for Animal Research at the University of California San Francisco (San Francisco, CA).

Immunohistochemistry, proliferation and apoptotic indices.

Antigen unmasking was achieved by placing the slides in a microwave oven on high for 10 min either in 10 mM sodium citrate buffer (pH 6.0) or 1mM *ethylenediaminetetraacetic acid* (EDTA; pH 8.5), followed by a 20-min cool down at room temperature. After a blocking step with the 5% goat serum and Avidin-Biotin blocking kit (Vector Laboratories, Burlingame, CA), the slides were incubated with primary antibodies overnight at 4°C. Slides were then subjected to 3% hydrogen peroxide for 10 min to quench endogenous peroxidase activity and, subsequently, the biotin-conjugated secondary antibody was applied at a 1:500

dilution for 30 min at room temperature. The primary antibodies against CK19 (Abcam, Cambridge, MA; 1:150), CCNE1 (Abcam; 1:100); phosphorylated/inactivated Rb (Ser807/8011; Cell Signaling Technology, Danvers, MA; 1:50); CDK4, cleaved caspase 3 (Cell Signaling Technology; 1:100), and Ki-67 (Thermo Fisher Scientific; 1:150) were used. Immunoreactivity was visualized with the Vectastain Elite ABC kit (Vector Laboratories, Burlingame, CA) and 3,3'- diaminobenzidine as the chromogen. Slides were counterstained with hematoxylin. Proliferation and apoptosis indices were determined in mouse ICC lesions by counting Ki-67 and Caspase 3 positive cells, respectively, on at least 3000 tumor cells per mouse sample.

Human Tissue Samples.

A collection of frozen ICC samples (n=32) was used in the present study. The clinicopathological features of liver cancer patients are summarized in Supplementary Table 1. ICC specimens were collected at the Medical Universities of Greifswald (Greifswald, Germany) and Sassari (Sassari, Italy). Institutional Review Board approval was obtained at the local Ethical Committee of the Medical Universities of Greifswald and Sassari. Informed consent was obtained from all subjects.

Statistical analysis.

GraphPad Prism version 6.0 (GraphPad Software Inc., La Jolla, CA) was used to evaluate statistical significance by Tukey–Kramer test. Data are presented as Means ± SD. Comparisons between two groups were performed with two-tailed unpaired t test. P values < 0.05 were considered statistically significant.

Results

Activation of the CDK4/6 pathway in human ICC

First, we evaluated the importance of the CDK4/6 pathway in human ICC specimens. Thus, we assessed the levels of *Rb1*, *CDK4*, *CDK6* as well as of *E2F1* and the E2F1 specific target *Cyclin E* (*CCNE1*) in a collection of human ICC samples and corresponding non-cancerous surrounding livers by qRT-PCR (Figure 1A). Of note, a strong upregulation of *CDK4/6*, *E2F1*, and *CCNE1* expression was detected in ICC specimens when compared with non-neoplastic counterparts. In addition, *Rb1* levels were significantly higher in tumors when compared with non-tumorous livers. Furthermore, higher levels of CDK4/6, Rb, phosphorylated/inactivated Rb, and Cyclin E were observed at the protein level using Western blotting in the same sample collection (Figure 1B and Supplementary Figure 1). The results were further confirmed by immunohistochemical staining on the same specimens. Indeed, increased nuclear immunoreactivity for phosphorylated/inactivated Rb, CDK4, and CCNE1 was detected in 81.2%, 78.1%, and 87.5% ICC samples, respectively, when compared with corresponding non-tumorous liver tissues (n=32; Figure 1C). Subsequently, the *Rb1, CDK4*, *CDK6, E2F1,* and *CCNE1* mRNA expression data were retrieved from TCGA, (frozen on 2/25/2015; and consisting of surgically resected 36 ICCs and 59 surrounding non-tumorous liver tissues(29,30) and NCI (from NCBI GEO website: GSE26566; consisting of 104 ICC and 59 non-neoplastic liver tissues; (29,30) datasets. Both datasets showed a significant upregulation of *CDK4, E2F1*, and *CCNE1* mRNA levels in

human ICC specimens compared with surrounding non-cancerous livers (Supplementary Figure 2B and D-E). *Rb1* mRNA levels were also slightly upregulated in human ICC specimens when compared to non-tumorous counterparts (Supplementary Figure 2A), whereas the expression of *CDK6* in ICC was weakly upregulated only in the NCI database (Supplementary Figure 2C). The present findings emphasize the almost ubiquitous activation of the CDK4/6 pathway in ICC patients, thus potentially representing an effective target in this disease.

Palbociclib inhibits cell growth by cell cycle arrest in human ICC cell lines

Next, we used Palbobiclib, a CDK4/6 inhibitor, to investigate whether inhibition of the CDK4/6 pathway afftects ICC cell growth *in vitro*. For this purpose, eight ICC cell lines were treated with various concentrations of Palbociclib for 72 hours followed by BrdU based cell proliferation analysis. Noticeably, most ICC cells tested were rather sensitive to Palbociclib, with IC_{50} ranging between 0.11μM to 1.34μM (Supplementary Figure 3). As Palbociclib has been shown to inhibit tumor growth via inducing cell cycle arrest (6,13), we investigated the expression of cell cycle related proteins in response to Palbociclib treatment in the ICC cell lines (Figure 2A and Supplementary Figure 4A). Palbociclib effectively suppressed the levels of phosphorylated/inactivated retinoblastoma protein (p-Rb) in all cell lines tested. In addition, protein levels of cell cycle related proteins, including Cyclin A, B, E, and PCNA, were repressed in most cell lines, whereas CCND1 increased in Palbociclib treated cells. Cell cycle negative regulators, including p21 and p53, did not show consistent changes of expression in response to Palbociclib (Figure 2A and Supplementary Figure 4A).

Next, we investigated whether Palbociclib modulates the expression of major pathways regulating tumor growth, specifically, the PI3K/AKT/mTOR and Ras/MAPK cascades (Figure 2B and Supplementary Figure 4B). No consistent changes in protein expression patterns in the two signaling cascades were observed in Palbociclib-treated ICC cells, thus suggesting that these pathways do not represent major targets of Palbociclib in this tumor type.

Altogether, the data demonstrate that Palbociclib inhibits ICC cell growth *in vitro* by inducing cell cycle arrest and reactivating/dephosphorylating the Rb protein.

Cyclin D1 overexpression limits the anti-growth properties of Palbociclib in ICC cells

Interestingly, the *in vitro* data revealed an upregulation of Cyclin D1 (CCND1) in Palbociclib-treated ICC cell lines (Figure 2A). Previous studies showed that Palbocilcib treatment may lead to increased CCND1 protein levels by stabilization of CDK4/CCND1 complex (31,32). Our intriguing observation prompted us to hypothesize that induction of CCND1 might be a key mechanism whereby ICC cells continue to grow despite CDK4/CDK6 inhibition. Thus, we determined whether silencing of CCND1 enhances the sensitivity of human ICC cell lines to Palbociclib. For this purpose, the *CCND1* gene was suppressed via specific siRNA in KKU-M213 and SNU1196 cells, randomly selected from the panel of ICC cells (Supplementary Figure 5). Of note, concomitant silencing of *CCND1* and Palbociclib administration resulted in an increased anti-growth effect in both cell lines,

whereas inhibition of *CCND1* expression alone did not significantly modify the growth rate of the same cells (Supplementary Figure 5).

The present findings suggest that CCND1 induction might represent a major mechanism of resistance by ICC cells to the growth inhibitory effects of Palbociclib.

Expression of functional Rb is responsible for long-term cell growth inhibition in response to Palbociclib

Subsequently, we tested the hypothesis that Rb expression may be used as a biomarker for Palbociclib sensitivity. Thus, we analyzed Rb expression in the 8 ICC cell lines (Figure 3A). A significant negative correlation between Rb protein levels and IC50 against Palbociclib was detected (Supplementary Figure 6). As the growth inhibition assay was a short-term assay, with cell growth rate being analyzed 72 hours after addition of Palbociclib to the growth medium, we hypothesized that Rb levels might also affect the long-term growth inhibitory activity of Palbociclib. To validate this hypothesis, we performed colony formation assay, and the number of colonies was analyzed ~2 weeks after Palbociclib or solvent (DMSO) treatment (Figure 3B and Supplementary Figure 7). Consistent with BrdU based short-term proliferation assay, all 3 cell lines with low Rb expression (TGBC, OCUG-1 and KMCH) showed higher IC_{50} against Palbociclib, whereas the 5 cell lines with high Rb expression (KKU-M213, huCC-T1, SNU1196, MzChA-1, and RBE) showed low IC_{50} (Figure 3C and3D) in colony formation assays.

To further investigate whether Rb levels determine long-term growth sensitivity to Palbociclib, we silenced the *Rb1* gene in four cell lines (KKU-M213, huCC-T1, SNU1196 and MzChA-1) with a previously validated shRNA against Rb (shRb) (33). As expected, *Rb1* expression was efficiently inhibited in all shRb-transfected cells. In colony formation assays, Rb suppression conferred strong resistance to Palbociclib in the 4 cell lines tested (Figure 3E and Supplementary Figure 8). For instance, in KKU-M213 cells, Palbociclib treatment effectively inhibited cell proliferation of shRNA control (shCtr) but not shRb-treated cells (Figure 3E).

In summary, the present data suggest that depletion of Rb renders ICC cells resistant to Palbociclib.

Palbociclib synergizes with MLN0128 to inhibit ICC cell growth *in vitro*

Previously, we demonstrated that mTOR inhibitors, such as MLN0128, are valuable drugs for restraining ICC cell growth. However, MLN0128 was found to be effective in promoting cell apoptosis while displaying limited anti-proliferative capacity (21). Because Palbociclib is a strong cell cycle inhibitor (6,13), we hypothesized that it might synergize with MLN0128 to suppress ICC cell growth. Five ICC cell lines were treated with MLN0128 and Palbociclib, either alone or in combination. Intriguingly, concomitant treatment of ICC cells with MLN0128 and Palbociclib resulted in stronger growth inhibitory activity (Figure 4A and Supplementary Figure 9). Subsequently, the Chou-Talalay method was used to calculate the combination index (CI) (26,27). Strikingly, the CI value was lower than 1 in the four ICC cell lines when MLN0128 and Palbociclib were concomitantly administered (Figure 4B and

Supplementary Figure 10). These data indicate a synergistic, anti-proliferative effect of combining Palbociclib with MLN0128 on ICC cells.

At the cellular level, using FACS analysis, Palbociclib elicited cell cycle arrest, whereas MLN0128 had limited effect on cell cycle (Figure 4C and Supplementary Figure 11). Strikingly, combined Palbociclib and MLN0128 treatment resulted in nearly complete cell cycle arrest.

At the molecular level, Palbociclib/MLN0128 combination induced an additional decline of Rb phosphorylation, and decreased the levels of cyclin A, cyclin B, and PCNA proteins when compared to Palbociclib alone (Figure 4D and Supplementary Figure 12A). Noticeably, Palbociclib treatment alone triggered CCND1 induction, whereas combined Palbociclib/MLN0128 administration prevented this phenomenon. Moreover, CDK inhibitor proteins p21 and p16 were upregulated in the Palbociclib/MLN0128 combination treatment group in several ICC cell lines. As concerns the Ras/MAPK pathway, Palbociclib and MLN0128, either alone or in combination, did not show consistent effects on phosphorylated/activated (p-)ERK levels (Figure 4E and Supplementary Figure 12B). In contrast, MLN0128 alone was effective against the AKT/mTOR cascade, an effect that was augmented by the combination treatment (as evidenced by the strong decline of phosphorylated/activated (p-)RPS6 and phosphorylated/inactivated (p-)4EBP1) in ICC cell lines.

In conclusion, the data indicate that Palbociclib synergizes with MLN0128 to constrain ICC cell growth *in vitro*.

Combined Palbociclib/MLN0128 treatment leads to tumor regression in AKT/YapS127A mice

Recently, we established a new murine ICC model driven by activated AKT and Yap, two oncoproteins frequently activated in human ICC (AKT/YapS127A) (21). In particular, we found that the standard chemotherapy for human ICC, consisting of gemcitabine plus oxaliplatin, had limited therapeutic value in AKT/YapS127A ICC lesions, whereas treatment of MLN0128 resulted in stable disease in these mice (21). Here, we tested the therapeutic potential of Palbociclib, either alone or in combination with MLN0128, in AKT/YapS127A mice. Thus, AKT/YapS127A mice were monitored for tumor growth until 3.5 weeks post injection, when the tumor burden was moderate (average liver weight ~3.5g) (Figure 5A and5C). Subsequently, AKT/YapS127A mice were randomly separated into 5 cohorts. The first cohort was harvested as ‘pre-treatment’ group, while the remaining mice were treated with vehicle, Palbociclib, MLN0128, or Palbociclib/MLN0128 for additional 3 weeks. Using mouse total body weight as measurement of overall health stature of mice, we tested different combination concentration ratio and found that 100mg/kg Palbociclib (16) plus 0.5mg/kg MLN0128 was well-tolerated and this dose was used for successive *in vivo* studies. It should be underlined that the dose of MLN0128 was lower (0.5mg/kg) in the combination therapy than that in our previous report when MLN0128 was used as monotherapy (1mg/kg) (21). In the vehicle treated cohort, all mice developed lethal burden of tumor and had to be euthanized by 4.7 to 6.5 weeks post injection (Figure 5B). Liver tumors in Palbociclib or MLN0128 treated cohorts grew slowly, and only a portion of mice

developed high tumor burden and were euthanized before the end of experiments. Still, ~60% and 40% of mice survived after 3 weeks of treatment in Palbociclib and MLN0128 monotherapy cohorts, respectively (Figure 5B). In contrast, all Palbociclib/MLN0128-treated mice showed good health, and only small tumors developed (Figure 5B). Using total liver weight as the measurement of tumor burden, the vehicle cohort had the highest tumor burden. Palbociclib and MLN0128 monotherapy cohorts showed significantly lower tumor burden than vehicle-treated mice. Yet, mice subjected to single treatment with Palbociclib or MLN0128 exhibited higher tumor burden compared with the pre-treatment cohort, indicating that tumors subjected to monotherapy continued to grow despite the treatment (Figure 5C). Palbociclib/MLN0128-treated mice displayed the lowest tumor burden, even lower than that in the pre-treatment cohort (Figure 5C). Histopathological analysis revealed that liver tumors in all cohorts were pure ICC (Figure 5D), as confirmed by diffuse immunoreactivity for the biliary marker CK19 (Figure 5E). As expected, liver CK19-positive areas were smallest in the Palbociclib/MLN0128 group (Figure 5E).

Altogether, the data indicate that Palbociclib or MLN0128 monotherapy has moderate therapeutic efficacy against AKT/YapS127A ICC, whereas combined Palbociclib/MLN0128 treatment leads to tumor regression.

Combined Palbociclib/MLN0128 regimen strongly inhibits tumor cell proliferation *in vivo*

Since the *in vitro* findings indicate that combined Palbociclib/MLN0128 treatment strongly inhibits ICC cell proliferation, we investigated whether the tumor inhibitory activity induced by the combined therapy is driven by the same mechanism *in vivo*. Thus, we analyzed the proliferation indices in the 5 cohorts using Ki-67 immunohistochemistry. MLN0128 treatment had no impact on cell proliferation rate, in accordance with previous findings (21), whereas Palbociclib alone mildly (although significantly) inhibited tumor cell proliferation at the dose used in the study (Figure 5F). In striking contrast, combined Palbociclib/MLN0128 treatment profoundly decreased tumor cell proliferation (Figure 5F). No synergistic effect on apoptosis was observed in the Palbociclib/MLN0128-treated group (Supplementary Figure 13).

At the molecular level, consistent with the *in vitro* data, p-Rb levels were significantly downregulated in Palbociclib-treated liver tumors, being virtually undetectable in the Palbociclib/MLN0128-treated lesions (Figure 6A). Palbociclib and Palbociclib/MLN0128 treatment also led to decreased expression of PCNA and increased levels of p16. Importantly, Palbociclib monotherapy triggered the induction of CCND1, which was instead prevented by Palbociclib/MLN0128 treatment (Figure 6A and Supplementary Figure 14A). As concerns apoptosis-related proteins (Figure 6B and Supplementary Figure 14B), Palbociclib and MLN0128, alone or in combination, triggered the increase of activated/cleaved-Caspase 3 and 7 levels. Palbociclib and MLN0128 treatment did not affect Ras/MAPK activity, whereas the PI3K/AKT/mTOR cascade was efficiently inhibited by MLN0128 and Palbociclib/MLN0128 (Figure 6C and Supplementary Figure 14C). As in the *in vitro* studies, the combination treatment resulted in the most pronounced inhibition of p-RPS6 in AKT/YapS127A ICC tumor cells.

In summary, our findings demonstrate that combined Palbociclib/MLN0128 treatment strongly inhibits tumor cell proliferation, leading to tumor regression, in AKT/YapS127A mice.

Discussion

ICC is a highly fatal tumor with rising incidence and lacking effective therapies. Thus, novel and successful therapeutic approaches against ICC are urgently needed. The molecular pathogenesis of ICC is complex, involving multiple signaling pathways and molecular alterations that contribute to tumor cell proliferation, survival, migration, and metastasis (34,35). Given the complexity of the oncogenic mechanisms responsible for ICC development and progression, it is likely that combination therapies simultaneously targeting different key molecules might possess more pronounced antitumor efficacy. In agreement with this hypothesis, combination therapies have emerged as a promising anti-neoplastic strategy and are now widely used at the clinical level (36–38). In particular, combination therapies targeting multiple pathways might overcome molecular mechanisms of drug resistance in tumor cells when compared to monotherapy, and the lower dose used might reduce the drgu toxicity (38).

As a possible targetable signaling cascade, our analysis shows that the CDK4/6 axis is activated in most ICC patients. In particular, Rb is hyperphosphorylated (a reversible event), but only rarely downregulated, in human ICC. This important evidence, together with previous data showing very rare genetic alterations of the *Rb1* gene in human ICC (18), indicate that the large majority of ICC patients could positively respond to treatments aimed at suppressing the CDK4/6 proteins.

In a previous investigation, we reported that the dual mTOR inhibitor MLN0128 displays a significant growth inhibitory activity in both human ICC cell lines and the AKT/YapS127A ICC mouse model, primarily via inducing apoptosis (21). However, MLN0128 failed to repress the sustained proliferation characteristic of AKT/YapS127A mice, thus resulting finally in decreased growth pace but not regression of ICC lesions. In light of these findings, we postulated that the persistent proliferation should be hampered in order to achieve effective tumor regression in AKT/YapS127A mice. Thus, to hinder AKT/YapS127A-dependent proliferation, we applied the CDK4/6 inhibitor Palbociclib, a strong cytostatic agent (6,13–16), in association with MLN0128. As hypothesized, we show here that combined treatment with Palbociclib and MLN0128 induces a more pronounced ICC growth inhibition compared to monotherapies, both *in vitro* and *in vivo*. Based on the results from the present report, it can be envisaged that this combination treatment might represent a potential new therapy for ICC. To the best of our knowledge, this is the first study showing a therapeutic effect of Palbociclib (alone and in combination with MLN0128) in ICC.

The importance of the functional crosstalk between CDK4/6 and mTOR inhibitors in cancer is underscored by a body of experimental evidence. For instance, it has been shown that mTOR activation is sufficient to render cells resistant to CDK4/6 inhibitors, while mTOR suppression greatly improves the Palbociclib anti-growth properties in pancreatic cancer (39). In particular, Palbociclib was found to sensitize pancreatic cancer cells to mTOR

inhibitors as well as to enhance its own anti-growth function via a positive feedback loop (39). Likewise, here we show that MLN0128 administration further augments the cytostatic function over ICC cells by Palbociclib that, in parallel, promotes MLN0128 anti-mTOR activity. Indeed, although Palbociclib alone has no obvious suppressive effects on mTOR in ICC cells, the present data indicate that Palbociclib sensitizes ICC cells to mTOR inhibition by MLN0128, with consequent more pronounced downregulation of mTOR downstream effectors. This effect might increase the anti-proliferative capacity of Palbociclib in ICC cells. In breast cancer cell lines, it has been found that they rapidly adapt to CDK4/6 inhibition by induction of CCND1. Once again, such a resistance was successfully prevented by concomitant administration of PI3K/AKT/mTOR inhibitors (40). Noticeably, our present data indicate that CCND1 upregulation is a mechanism of resistance to CDK4/6 blockade also in ICC cells, and this event can be circumvented by mTOR inhibition. Thus, it is tempting to speculate that induction of CCND1 and/or the PI3K/AKT/mTOR pathway might be a major mechanism of resistance in multiple cancer types that should be considered (and prevented) when administering CDK4/6 inhibitors to patients.

In summary, the present investigation indicates that the CDK4/6 axis and the mTOR pathway are concurrently induced and functionally interact in ICC to sustain unrestrained proliferation of cancer cells. Combined suppression of the two pathways is highly detrimental for ICC growth *in vitro* and *in vivo* and prevents acquired tumor cell resistance to monotherapy. Thus, our data strongly support further clinical evaluation of combination therapies with CDK4/6 and mTOR inhibitors for the treatment of human ICC.

Supplementary Material

Refer to Web version on PubMed Central for supplementary material.

Acknowledgments:

We would like to thank Dr. Gregory J. Gores at Mayo Clinic for providing the huCC-T1 cell line.

Financial Support statement: This work is supported by NIH grants R01CA136606 and R01CA190606 to XC; P30DK026743 for UCSF Liver Center; China Scholarship Council (201506350124) to XS; National Natural Science Foundation of China (NSFC) (31671945) to HH.

List of Abbreviations:

AKT	v-akt murine thymoma viral oncogene homolog
CCND1	cyclin D1
CDK	cyclin-dependent kinase
ICC	intrahepatic cholangiocarcinoma
mTOR	mammalian target of rapamycin
Rb	retinoblastoma
Yap	Yes-associated protein

References:

1. Bridgewater J, Galle PR, Khan SA, Llovet JM, Park JW, Patel T, et al. Guidelines for the diagnosis and management of intrahepatic cholangiocarcinoma. Journal of hepatology 2014;60(6):1268–89 doi 10.1016/j.jhep.2014.01.021. [PubMed: 24681130]
2. Razumilava N, Gores GJ. Cholangiocarcinoma. Lancet (London, England) 2014;383(9935):2168–79 doi 10.1016/s0140-6736(13)61903-0.
3. Rizvi S, Gores GJ. Emerging molecular therapeutic targets for cholangiocarcinoma. Journal of hepatology 2017;67(3):632–44 doi 10.1016/j.jhep.2017.03.026. [PubMed: 28389139]
4. Rahnemai-Azar AA, Weisbrod A, Dillhoff M, Schmidt C, Pawlik TM. Intrahepatic cholangiocarcinoma: Molecular markers for diagnosis and prognosis. Surgical oncology 2017;26(2):125–37 doi 10.1016/j.suronc.2016.12.009. [PubMed: 28577718]
5. Konstantinidis IT, Groot Koerkamp B, Do RK, Gonen M, Fong Y, Allen PJ, et al. Unresectable intrahepatic cholangiocarcinoma: Systemic plus hepatic arterial infusion chemotherapy is associated with longer survival in comparison with systemic chemotherapy alone. Cancer 2016;122(5):758–65 doi 10.1002/cncr.29824. [PubMed: 26695839]
6. Asghar U, Witkiewicz AK, Turner NC, Knudsen ES. The history and future of targeting cyclin-dependent kinases in cancer therapy. Nature reviews Drug discovery 2015;14(2):130–46 doi 10.1038/nrd4504. [PubMed: 25633797]
7. Malumbres M, Barbacid M. To cycle or not to cycle: a critical decision in cancer. Nature reviews Cancer 2001;1(3):222–31 doi 10.1038/35106065. [PubMed: 11902577]
8. Whittaker SR, Mallinger A, Workman P, Clarke PA. Inhibitors of cyclin-dependent kinases as cancer therapeutics. Pharmacology & therapeutics 2017;173:83–105 doi 10.1016/j.pharmthera.2017.02.008. [PubMed: 28174091]
9. Satyanarayana A, Kaldis P. Mammalian cell-cycle regulation: several Cdks, numerous cyclins and diverse compensatory mechanisms. Oncogene 2009;28(33):2925–39 doi 10.1038/onc.2009.170. [PubMed: 19561645]
10. Bertoli C, Skotheim JM, de Bruin RA. Control of cell cycle transcription during G1 and S phases. Nature reviews Molecular cell biology 2013;14(8):518–28 doi 10.1038/nrm3629. [PubMed: 23877564]
11. Malumbres M, Barbacid M. Cell cycle, CDKs and cancer: a changing paradigm. Nature reviews Cancer 2009;9(3):153–66 doi 10.1038/nrc2602. [PubMed: 19238148]
12. Otto T, Sicinski P. Cell cycle proteins as promising targets in cancer therapy. Nature reviews Cancer 2017;17(2):93–115 doi 10.1038/nrc.2016.138. [PubMed: 28127048]
13. Sherr CJ, Beach D, Shapiro GI. Targeting CDK4 and CDK6: From Discovery to Therapy. Cancer discovery 2016;6(4):353–67 doi 10.1158/2159-8290.cd-15-0894. [PubMed: 26658964]
14. Hamilton E, Infante JR. Targeting CDK4/6 in patients with cancer. Cancer treatment reviews 2016;45:129–38 doi 10.1016/j.ctrv.2016.03.002. [PubMed: 27017286]
15. O'Leary B, Finn RS, Turner NC. Treating cancer with selective CDK4/6 inhibitors. Nature reviews Clinical oncology 2016;13(7):417–30 doi 10.1038/nrclinonc.2016.26.
16. Bollard J, Miguela V, Ruiz de Galarreta M, Venkatesh A, Bian CB, Roberto MP, et al. Palbociclib (PD-0332991), a selective CDK4/6 inhibitor, restricts tumour growth in preclinical models of hepatocellular carcinoma. Gut 2017;66(7):1286–96 doi 10.1136/gutjnl-2016-312268. [PubMed: 27849562]
17. Walker AJ, Wedam S, Amiri-Kordestani L, Bloomquist E, Tang S, Sridhara R, et al. FDA Approval of Palbociclib in Combination with Fulvestrant for the Treatment of Hormone Receptor-Positive, HER2-Negative Metastatic Breast Cancer. Clinical cancer research : an official journal of the American Association for Cancer Research 2016;22(20):4968–72 doi 10.1158/1078-0432.ccr-16-0493. [PubMed: 27407089]
18. Ma MKF, Lau EYT, Leung DHW, Lo J, Ho NPY, Cheng LKW, et al. Stearoyl-CoA desaturase regulates sorafenib resistance via modulation of ER stress-induced differentiation. Journal of hepatology 2017;67(5):979–90 doi 10.1016/j.jhep.2017.06.015. [PubMed: 28647567]
19. Saxton RA, Sabatini DM. mTOR Signaling in Growth, Metabolism, and Disease. Cell 2017;168(6):960–76 doi 10.1016/j.cell.2017.02.004. [PubMed: 28283069]

20. Fan B, Malato Y, Calvisi DF, Naqvi S, Razumilava N, Ribback S, et al. Cholangiocarcinomas can originate from hepatocytes in mice. The Journal of clinical investigation 2012;122(8):2911–5 doi 10.1172/jci63212. [PubMed: 22797301]
21. Zhang S, Song X, Cao D, Xu Z, Fan B, Che L, et al. Pan-mTOR inhibitor MLN0128 is effective against intrahepatic cholangiocarcinoma in mice. Journal of hepatology 2017 doi 10.1016/j.jhep.2017.07.006.
22. Ghobrial IM, Siegel DS, Vij R, Berdeja JG, Richardson PG, Neuwirth R, et al. TAK-228 (formerly MLN0128), an investigational oral dual TORC1/2 inhibitor: A phase I dose escalation study in patients with relapsed or refractory multiple myeloma, non-Hodgkin lymphoma, or Waldenstrom's macroglobulinemia. American journal of hematology 2016;91(4):400–5 doi 10.1002/ajh.24300. [PubMed: 26800393]
23. Hu J, Che L, Li L, Pilo MG, Cigliano A, Ribback S, et al. Co-activation of AKT and c-Met triggers rapid hepatocellular carcinoma development via the mTORC1/FASN pathway in mice. Scientific reports 2016;6:20484 doi 10.1038/srep20484. [PubMed: 26857837]
24. Marti P, Stein C, Blumer T, Abraham Y, Dill MT, Pikiolek M, et al. YAP promotes proliferation, chemoresistance, and angiogenesis in human cholangiocarcinoma through TEAD transcription factors. Hepatology (Baltimore, Md) 2015;62(5):1497–510 doi 10.1002/hep.27992.
25. Tao J, Calvisi DF, Ranganathan S, Cigliano A, Zhou L, Singh S, et al. Activation of beta-catenin and Yap1 in human hepatoblastoma and induction of hepatocarcinogenesis in mice. Gastroenterology 2014;147(3):690–701 doi 10.1053/j.gastro.2014.05.004. [PubMed: 24837480]
26. Chou TC. Theoretical basis, experimental design, and computerized simulation of synergism and antagonism in drug combination studies. Pharmacological reviews 2006;58(3):621–81 doi 10.1124/pr.58.3.10. [PubMed: 16968952]
27. Chou TC, Talalay P. Quantitative analysis of dose-effect relationships: the combined effects of multiple drugs or enzyme inhibitors. Advances in enzyme regulation 1984;22:27–55. [PubMed: 6382953]
28. Yue S, Li J, Lee SY, Lee HJ, Shao T, Song B, et al. Cholesteryl ester accumulation induced by PTEN loss and PI3K/AKT activation underlies human prostate cancer aggressiveness. Cell metabolism 2014;19(3):393–406 doi 10.1016/j.cmet.2014.01.019. [PubMed: 24606897]
29. Andersen JB, Spee B, Blechacz BR, Avital I, Komuta M, Barbour A, et al. Genomic and genetic characterization of cholangiocarcinoma identifies therapeutic targets for tyrosine kinase inhibitors. Gastroenterology 2012;142(4):1021–31 e15 doi 10.1053/j.gastro.2011.12.005. [PubMed: 22178589]
30. Farshidfar F, Zheng S, Gingras MC, Newton Y, Shih J, Robertson AG, et al. Integrative Genomic Analysis of Cholangiocarcinoma Identifies Distinct IDH-Mutant Molecular Profiles. Cell reports 2017;19(13):2878–80 doi 10.1016/j.celrep.2017.06.008. [PubMed: 28658632]
31. Comstock CE, Augello MA, Goodwin JF, de Leeuw R, Schiewer MJ, Ostrander WF, Jr., et al. Targeting cell cycle and hormone receptor pathways in cancer. Oncogene 2013;32(48):5481–91 doi 10.1038/onc.2013.83. [PubMed: 23708653]
32. Dean JL, Thangavel C, McClendon AK, Reed CA, Knudsen ES. Therapeutic CDK4/6 inhibition in breast cancer: key mechanisms of response and failure. Oncogene 2010;29(28):4018–32 doi 10.1038/onc.2010.154. [PubMed: 20473330]
33. Kim KJ, Godarova A, Seedle K, Kim MH, Ince TA, Wells SI, et al. Rb suppresses collective invasion, circulation and metastasis of breast cancer cells in CD44-dependent manner. PloS one 2013;8(12):e80590 doi 10.1371/journal.pone.0080590. [PubMed: 24324613]
34. Chen MH, Chiang KC, Cheng CT, Huang SC, Chen YY, Chen TW, et al. Antitumor activity of the combination of an HSP90 inhibitor and a PI3K/mTOR dual inhibitor against cholangiocarcinoma. Oncotarget 2014;5(9):2372–89 doi 10.18632/oncotarget.1706. [PubMed: 24796583]
35. Blechacz B Cholangiocarcinoma: Current Knowledge and New Developments. Gut and liver 2017;11(1):13–26 doi 10.5009/gnl15568. [PubMed: 27928095]
36. Shen S, Liu M, Li T, Lin S, Mo R. Recent progress in nanomedicine-based combination cancer therapy using a site-specific co-delivery strategy. Biomaterials science 2017;5(8):1367–81 doi 10.1039/c7bm00297a. [PubMed: 28664207]

37. Qiao M, Jiang T, Ren S, Zhou C. Combination Strategies on the Basis of Immune Checkpoint Inhibitors in Non-Small-Cell Lung Cancer: Where Do We Stand? Clinical lung cancer 2017 doi 10.1016/j.cllc.2017.06.005.

38. Kerru N, Singh P, Koorbanally N, Raj R, Kumar V. Recent advances (2015–2016) in anticancer hybrids. European journal of medicinal chemistry 2017 doi 10.1016/j.ejmech.2017.07.033.

39. Heilmann AM, Perera RM, Ecker V, Nicolay BN, Bardeesy N, Benes CH, et al. CDK4/6 and IGF1 receptor inhibitors synergize to suppress the growth of p16INK4A-deficient pancreatic cancers. Cancer research 2014;74(14):3947–58 doi 10.1158/0008-5472.can-13-2923. [PubMed: 24986516]

40. Herrera-Abreu MT, Palafox M, Asghar U, Rivas MA, Cutts RJ, Garcia-Murillas I, et al. Early Adaptation and Acquired Resistance to CDK4/6 Inhibition in Estrogen Receptor-Positive Breast Cancer. Cancer research 2016;76(8):2301–13 doi 10.1158/0008-5472.can-15-0728. [PubMed: 27020857]

Translational Relevance

Intrahepatic cholangiocarcinoma (ICC) is a highly aggressive liver tumor, with limited treatment options and no FDA-approved targeted therapy. Here, we show for the first time that combining pan-mTOR and CDK4/6 inhibitors synergizes to remarkably restrain the growth of ICC cells *in vitro* and to induce tumor regression in an ICC preclinical mouse model *in vivo*. Mechanistically, we demonstrate that combined treatment with pan-mTOR and CDK4/6 inhibitors triggers strong inhibition of cell proliferation in ICC cells *in vitro* and *in vivo*. At the molecular level, while the CDK4/6 inhibitor potentiates mTOR inhibitor's activity, the mTOR inhibitor prevents CDK4/6 inhibitor induced upregulation of cyclin D1. The present data have major translational implications, strongly supporting the implementation of the combination of pan-mTOR and CDK4/6 inhibitors in clinical trials for ICC treatment.

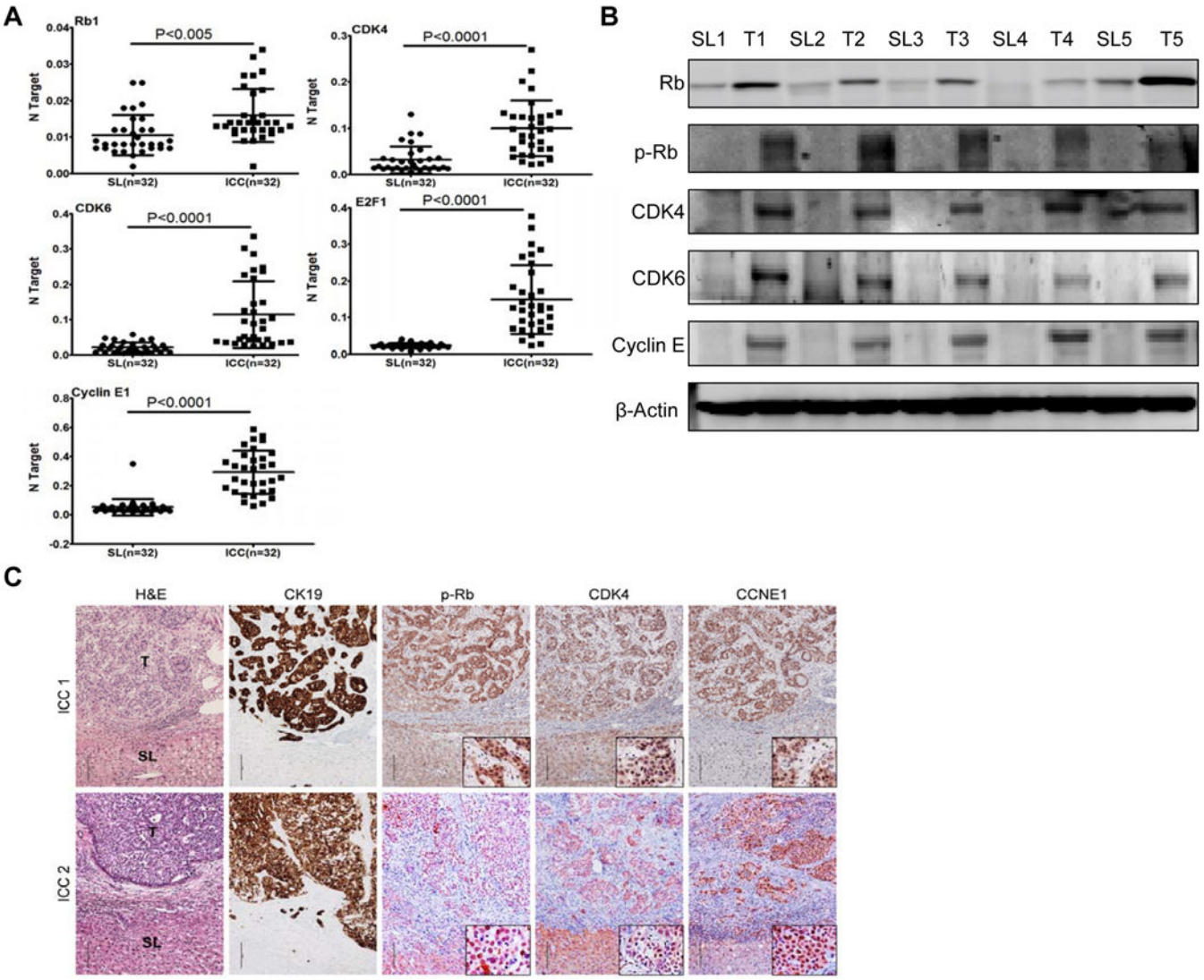

Figure 1. Activation of the CDK4/6 axis in human intrahepatic cholangiocarcinoma (ICC) specimens.

(A) qRT-PCR analysis of *Rb1*, *CDK4*, CDK6, E2F1, and Cyclin E1 mRNA levels in 32 paired human ICC and non-tumorous surrounding liver tissues (SL). (B) Representative Western blot analysis of Rb, phosphorylated/inactivated (p)-Rb, CDK4, CDK6, and Cyclin E in non-tumorous livers (SL) and ICC samples (n =32). β-Actin was used as loading control. (C) Representative immunohistochemical patterns of phosphorylated/inactivated retinoblastoma protein (p-Rb), CDK4, and Cyclin E1 (CCNE1) in two human intrahepatic cholangiocarcinoma (ICC1 and ICC2) specimens. While normal surrounding non-tumorous liver tissues (SL) exhibited faint or absent nuclear immunoreactivity for p-RB, CDK4, and CCNE1, the corresponding tumor part (T) showed strong nuclear immunolabeling for the same proteins. Nuclear immunoreactivity for the investigated proteins can be better appreciated at higher magnification (insets). CK19 staining indicates the biliary nature of ICC cells. In ICC2 immunohistochemistry (lower panels), the Vector NovaRED Peroxidase

Substrate was applied to intensify the signal. Magnification: 100X in whole pictures, 400X in insets; scale bar: 100μm.

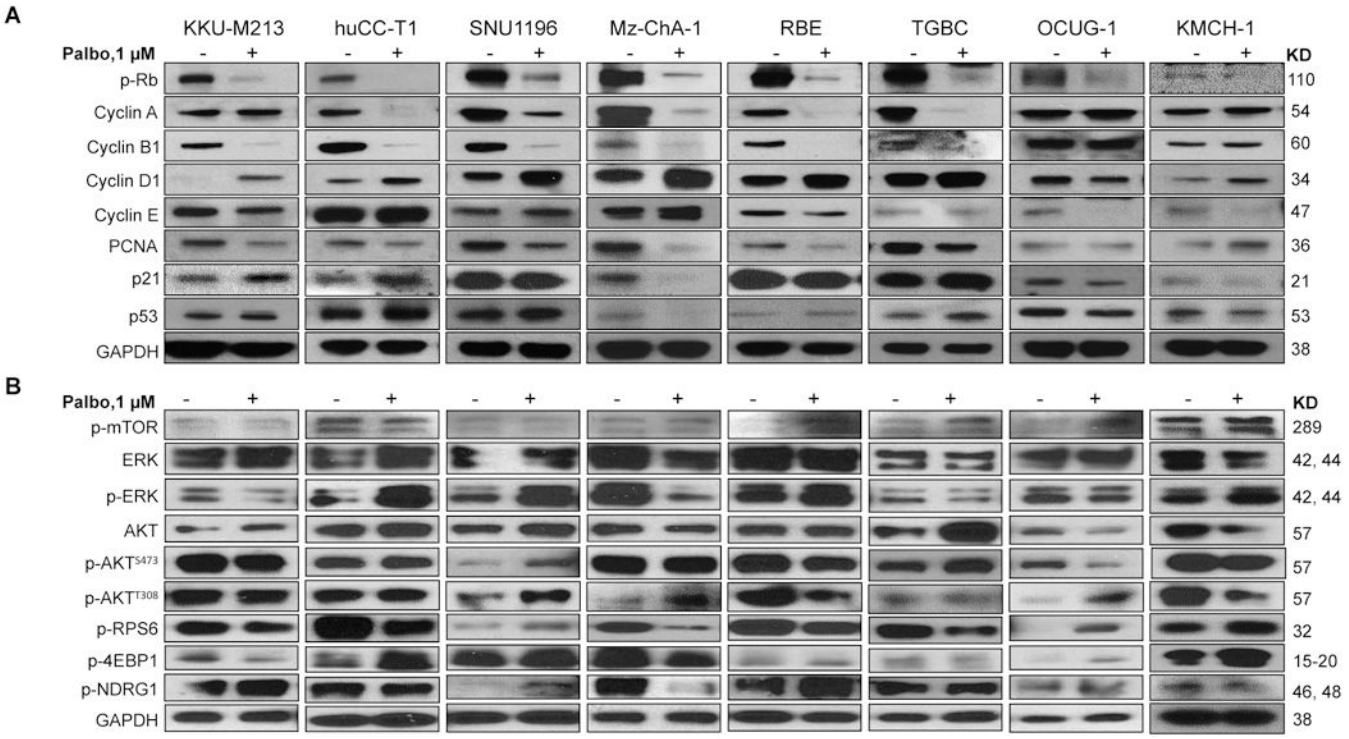

Figure 2. Effect of Palbociclib on the levels of putative target proteins in human ICC cell lines.

Western blot analysis of cell cycle related proteins (A) as well as AKT/mTOR and Ras/MAPK pathways (B) after treatment with the indicated doses of Palbociclib for 3 days in eight representative ICC cell lines. Abbreviations: Palbo, Palbociclib.

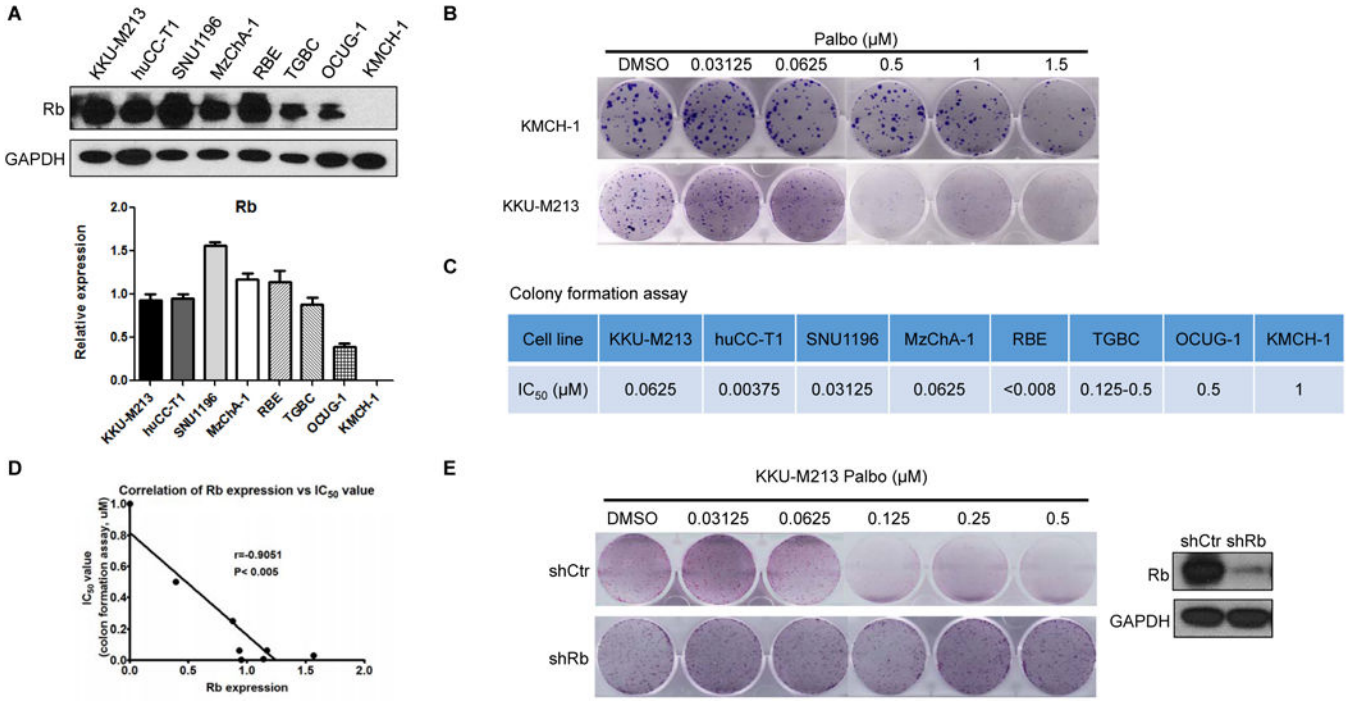

Cell line	KKU-M213	huCC-T1	SNU1196	MzChA-1	RBE	TGBC	OCUG-1	KMCH-1
IC_{50} (μM)	0.0625	0.00375	0.03125	0.0625	<0.008	0.125-0.5	0.5	1

Figure 3. Palbociclib inhibits ICC cell growth in a retinoblastoma (RB)-dependent manner *in vitro.*

(A) Western blot analysis of Rb in ICC cell lines. (B) Crystal violet staining of colonies from KMCH and KKU-M213 cell lines treated with the indicated doses of Palbociblib. (C) IC_{50} values calculated by quantifying the Crystal violet staining of colonies from eight ICC cell lines. (D) The correlation analysis of Rb expression and IC50 value after two weeks treatment of Palbociclib with the indicated doses of Palbociclib in human cholangiocarcinoma (ICC) cell lines. The data were analyzed using the Pearson correlation method. R and p value are presented on the graph. (E) Crystal violet staining of colonies in KKU-M213 cell line infected with shCtr or shRB. Abbreviations: shCtr, control; Palbo, Palbociclib; Rb, Retinoblastoma.

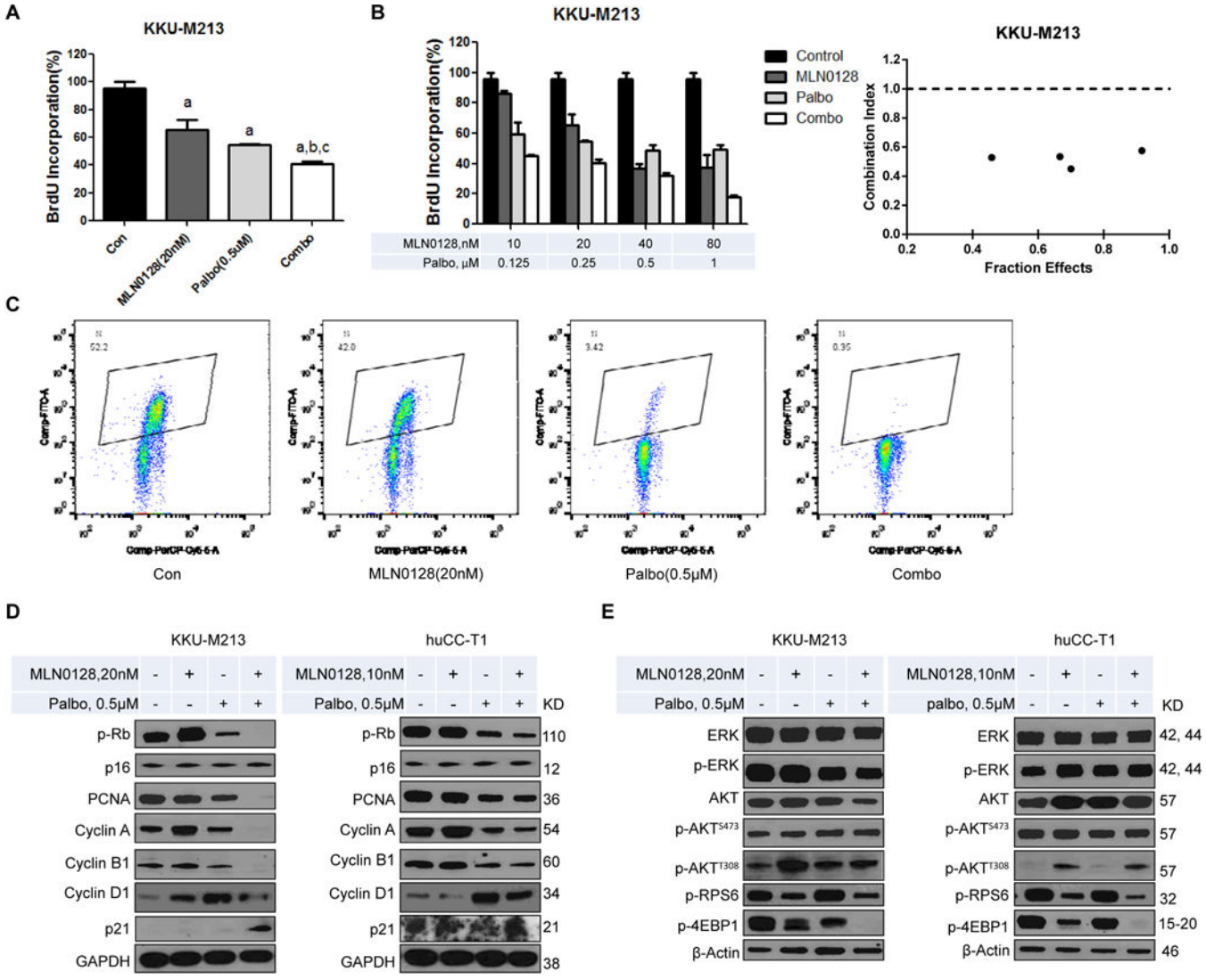

Figure 4. Effect of combined Palbociclib/MLN0128 treatment on ICC cell proliferation and cell cycle.

(A) Combining Palbociclib with MLN0128 resulted in reduced cell proliferation in KKU-M213 cell line. (B) The enhanced inhibitory effect of Palbociclib/MLN0128 combination on ICC *in vitro* growth is a synergistic action. (C) Enhanced cell cycle arrest in KKU-M213 cell line treated with Palbociclib plus MLN0128. The percentages of cells in the S phase are shown. (D) Representative Western Blot analysis of proliferation signaling pathways in KKU-M213 and huCC-T1 cell lines. (E) Representative Western blot analysis of AKT/mTOR and Ras/MAPK signaling pathways in KKU-M213 and huCC-T1 cell lines. Tukey–Kramer test: at least $P < 0.001$. a, vs control; b, vs MLN0128; c, vs Palbo; d, vs Combo. Abbreviations: Con, Control; Palbo, Palbociclib; Combo, combined Palbociclib/MLN0128 treatment.

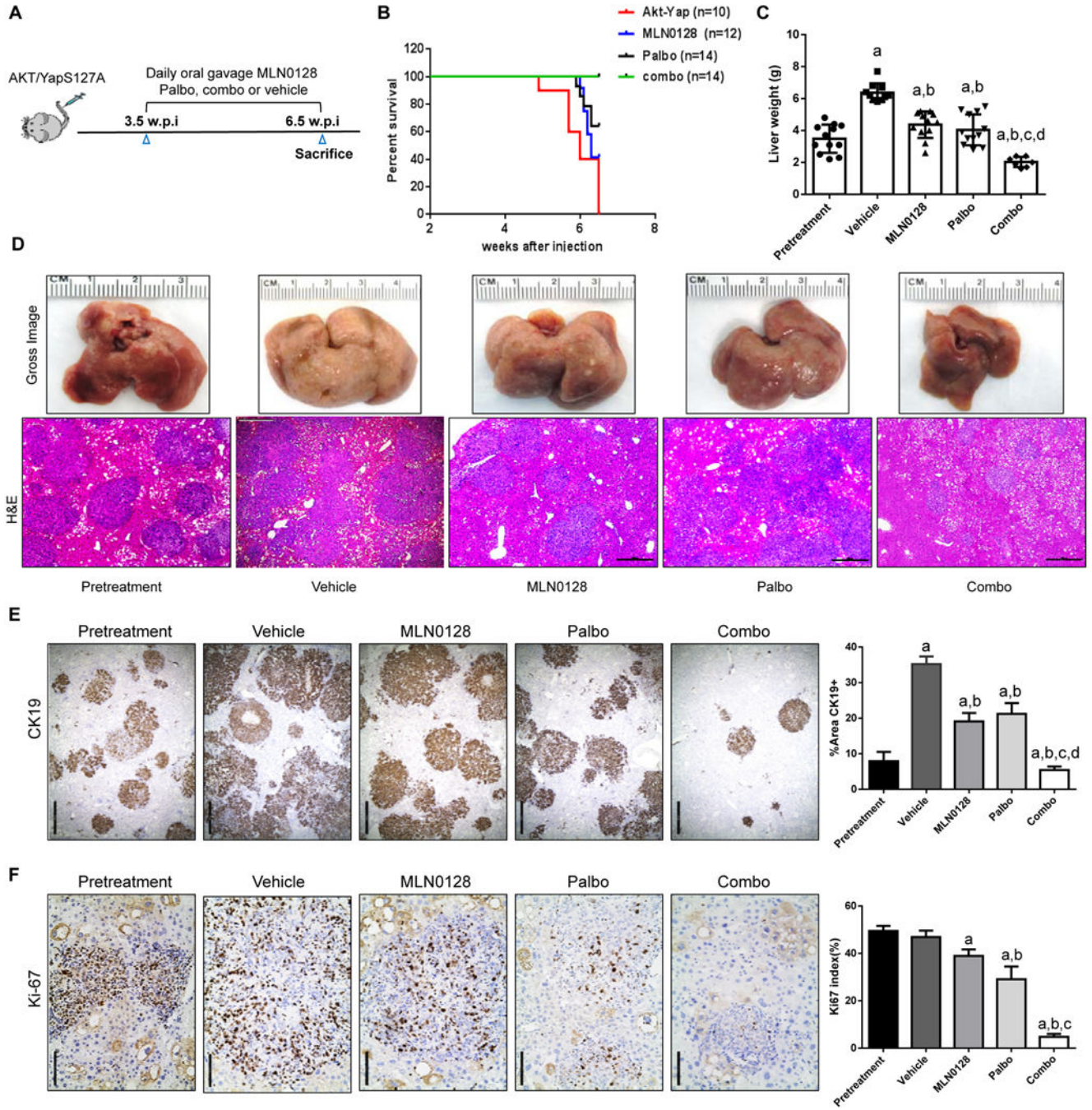

Figure 5. Palbociclib/MLN0128 combination has a potent anti-neoplastic effect in ICC lesions from AKT/YapS127A mice.

(A) Study design. (B) Survival curve of AKT/YapS127A mice pretreated and treated with MLN0128, Palbociclib, Palbociclib/MLN0128 and vehicle. (C) Liver weight of pretreatment, vehicle-, MLN0128-, Palbociclib-, and MLN0128/Palbociclib-treated AKT/YapS127A mice. (D) Gross images and H&E staining of livers from pretreatment, vehicle-, MLN0128-, Palbociclib-, and Palbociclib/MLN0128-treated AKT/YapS127A mice. (Magnification: 100X, Scale bar: 200μm). (E) CK19 (Magnification: 40X, Scale bar: 500μm). and (F) Ki-67 (Magnification: 200X, Scale bar: 100μm) staining in livers from

AKT/YapS127A mice subjected to the various treatments. CK19 staining was quantified and represented as the percentage of the positive staining area of the whole section area. Ki-67 positive cells were counted and quantified as proliferation index. Tukey–Kramer test: at least $P < 0.001$. a, vs Pretreatment; b, vs Vehicle; c, vs MLN0128; d, vs Palbo; e, vs Combo. Abbreviations: Palbo, Palbociclib; Combo, combined Palbociclib/MLN0128 treatment.

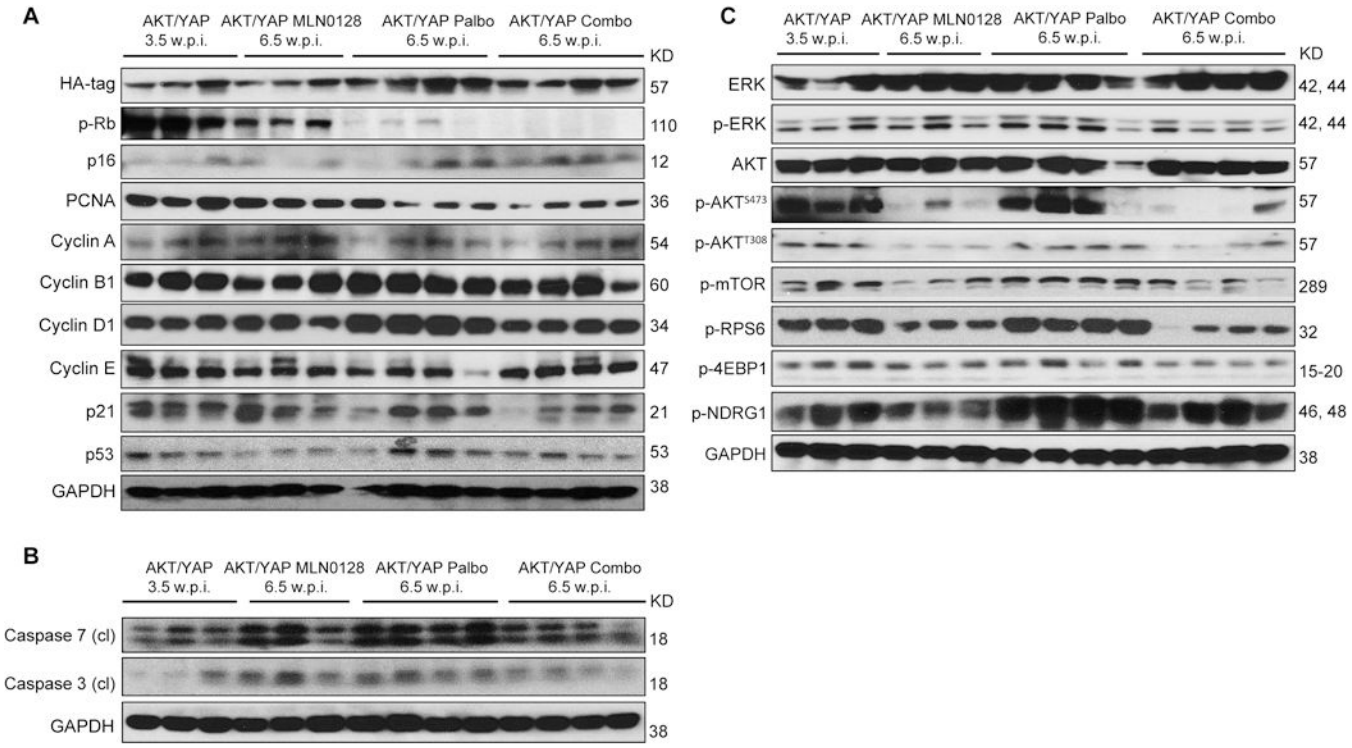

Figure 6. Effect of Palbociclib/MLN0128 treatment on the levels of putative target proteins in livers from AKT/YapS127A mice.

Western blot analysis was performed to analyze proliferation (A), apoptosis (B) as well as AKT/mTOR and Ras/MAPK (C) pathways in ICC tissues from pretreatment, vehicle-, MLN0128-, Palbo-, and Palbo/MLN0128-treated AKT/YapS127A mice. Abbreviations: Palbo, Palbociclib; Combo, combined Palbociclib/MLN0128 treatment.